Electroweak Symmetry Non-restoration in UV-complete Models with New Fermions

Yu Hang Ng

Department of Physics and Astronomy
University of Nebraska-Lincoln

2021 Phenomenology Symposium

May 25, 2021

INTRODUCTION

Electroweak symmetry is restored at high temperature in Standard Model and most of the BSM theories. For examples,

1. SM:
$$\frac{\partial^2 V_1^{th}}{\partial h^2}\Big|_{h=0} = T^2\left(\frac{3}{16}g^2 + \frac{1}{16}g'^2 + \frac{1}{4}\lambda_t^2 + \frac{1}{2}\lambda\right)$$
2. SM + real singlet scalar ($\mathbb{Z}_2$):
$$\frac{\partial^2 V_1^{th}}{\partial h^2}\Big|_{h=0} = T^2\left(\frac{3}{16}g^2 + \frac{1}{16}g'^2 + \frac{1}{4}\lambda_t^2 + \frac{1}{2}\lambda + \frac{1}{12}\lambda_{hs}\right)$$

EWSNR VIA NEW SCALARS

In some models, Electroweak symmetry was always broken (SNR) or only temporary restored (TR).

1. SM + singlet scalar s_i with $O(N_s)$ global symmetry (Meade & Ramani,1807.07578):

$$V = V_{SM} + \frac{1}{2}\mu_s^2(s_i s_i) + \frac{1}{4}\lambda_s(s_i s_i)^2 + \frac{1}{2}\lambda_{hs}h^2(s_i s_i)$$

$$\left.\frac{\partial^2 V_1^{th}}{\partial h^2}\right|_{h=0} = T^2\left(\frac{3}{16}g^2 + \frac{1}{16}g'^2 + \frac{1}{4}\lambda_t^2 + \frac{1}{2}\lambda + \frac{N_s}{12}\lambda_{hs}\right)$$

EWSNR VIA NEW SCALARS

In some models, Electroweak symmetry was always broken (SNR) or only temporary restored (TR).

1. SM + singlet scalar s_i with $O(N_s)$ global symmetry (Meade & Ramani,1807.07578):

$$V = V_{SM} + \frac{1}{2}\mu_s^2(s_i s_i) + \frac{1}{4}\lambda_s(s_i s_i)^2 + \frac{1}{2}\lambda_{hs}h^2(s_i s_i)$$

$$\left.\frac{\partial^2 V_1^{th}}{\partial h^2}\right|_{h=0} = T^2\left(\frac{3}{16}g^2 + \frac{1}{16}g'^2 + \frac{1}{4}\lambda_t^2 + \frac{1}{2}\lambda + \frac{N_s}{12}\lambda_{hs}\right)$$

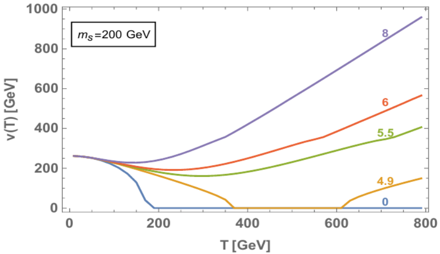

Temperature dependent vev for different values of $N_s|\lambda_{hs}|$.

EWSNR VIA NEW SCALARS

In some models, Electroweak symmetry was always broken (SNR) or only temporary restored (TR).

1. SM + singlet scalar s_i with $O(N_s)$ global symmetry (Meade & Ramani,1807.07578):

$$V = V_{SM} + \frac{1}{2}\mu_s^2(s_i s_i) + \frac{1}{4}\lambda_s(s_i s_i)^2 + \frac{1}{2}\lambda_{hs}h^2(s_i s_i)$$

$$\frac{\partial^2 V_1^{th}}{\partial h^2}\Big|_{h=0} = T^2\left(\frac{3}{16}g^2 + \frac{1}{16}g'^2 + \frac{1}{4}\lambda_t^2 + \frac{1}{2}\lambda + \frac{N_s}{12}\lambda_{hs}\right)$$

2. SM + Inert Higgs Doublet + singlet scalar($O(N_s)$) (Carena et al.,2104.00638)

3. 2HDM + real singlet scalar (Heinemeyer et at.,2103.12707)

EWSNR VIA NEW SCALARS

In some models, Electroweak symmetry was always broken (SNR) or only temporary restored (TR).

1. SM + singlet scalar s_i with $O(N_s)$ global symmetry (Meade & Ramani,1807.07578):

$$V = V_{SM} + \frac{1}{2}\mu_s^2(s_i s_i) + \frac{1}{4}\lambda_s(s_i s_i)^2 + \frac{1}{2}\lambda_{hs}h^2(s_i s_i)$$

$$\left.\frac{\partial^2 V_1^{th}}{\partial h^2}\right|_{h=0} = T^2\left(\frac{3}{16}g^2 + \frac{1}{16}g'^2 + \frac{1}{4}\lambda_t^2 + \frac{1}{2}\lambda + \frac{N_s}{12}\lambda_{hs}\right)$$

2. SM + Inert Higgs Doublet + singlet scalar($O(N_s)$) (Carena et al.,2104.00638)
3. 2HDM + real singlet scalar (Heinemeyer et at.,2103.12707)

Is it possbile to achive SNR or TR for EW symmetry by adding new fermions to SM?

EWSNR VIA NEW FERMIONS

In high temperature limit (i.e. when $m_i^2 \ll T^2$) , (Matsedonskyi,Servant, 2002.05174)

$$\left.\frac{\partial^2 V_{1,F}^{th}}{\partial h^2}\right|_{h=0} = \sum_i T^2 \frac{n_F}{48} \frac{\partial^2 m_i^2}{\partial h^2} = T^2 \frac{n_F}{48} \frac{\partial^2}{\partial h^2} \sum_i m_i^2$$
$$= T^2 \frac{n_F}{48} \frac{\partial^2}{\partial h^2} \mathrm{Tr}\left(M_f^\dagger M_f\right) = T^2 \frac{n_F}{48} \frac{\partial^2}{\partial h^2} \sum_{i,j} |M_{ij}|^2$$

In renormalizable models, $M_{ij} = a_0 + a_1 h$, hence $\left.\frac{\partial^2 V_{1,F}^{th}}{\partial h^2}\right|_{h=0} \geq 0$. Thus, it is impossible to achieve EWSNR by adding new fermions!

SINGLET-DOUBLET MODEL

$$L_{L,R} = \begin{bmatrix} N \\ E \end{bmatrix}_{L,R} \sim (1,2)_{-\frac{1}{2}},\ N'_{L,R} \sim (1,1)_0$$

$$\begin{aligned} \mathcal{L}^i_{mass} &= -y_1 \overline{L_L} \widetilde{\phi} N'_R - y_2 \overline{N'_L} \widetilde{\phi}^\dagger L_R - m_L \overline{L_L} L_R - m_{N'} \overline{N'_L} N'_R + h.c. \\ &= -\overline{F_L} M F_R \end{aligned}$$

$$F_{L,R} = \begin{bmatrix} N' \\ N \\ E \end{bmatrix}, \quad M = \begin{bmatrix} m_{N'} & m_{NN'2} & 0 \\ m_{NN'1} & m_L & 0 \\ 0 & 0 & m_L \end{bmatrix}, \quad m_{NN'i} = y_i h/\sqrt{2},$$

$$\phi = \begin{bmatrix} G^+ \\ (h + iG^0)/\sqrt{2} \end{bmatrix}, \quad \widetilde{\phi} = i\sigma_2 \phi^*.$$

The mass matrix can be diagonalized by biunitary transformation. The physical masses are m_L, m_{N1}, m_{N2}.

$$m_{N1}^2 = \frac{1}{2}\left(A_N^2 - \sqrt{\left(A_N^2\right)^2 - 4\left(\Delta_N^2\right)^2}\right)$$

$$m_{N2}^2 = \frac{1}{2}\left(A_N^2 + \sqrt{\left(A_N^2\right)^2 - 4\left(\Delta_N^2\right)^2}\right)$$

where

$$A_N^2 = |m_{NN'1}|^2 + |m_{NN'2}|^2 + |m_{N'}|^2 + |m_L|^2$$

$$\Delta_N^2 = |m_L m_{N'} - m_{NN'1} m_{NN'2}|$$

$$\left.\frac{\partial^2 V_{1,F}^{th}}{\partial h^2}\right|_{h=0} = \frac{T^2}{12}\frac{\partial^2}{\partial h^2}\sum_{N1,N2,L} m_i^2 > 0$$

What if the heavier fermion (N_2) is decoupled from the thermal bath?

When $m_L^2 \gg m_{N'}^2,\ \frac{1}{2}|y_1 y_2| h^2,\ T^2$,

$$m_{N1}^2 \approx m_{N'}^2 - \frac{m_{N'}\,\mathrm{Re}(y_1 y_2)}{m_L} h^2, \quad m_{N2}^2 \approx m_L^2 + \frac{m_{N'}\,\mathrm{Re}(y_1 y_2)}{m_L} h^2$$

$$\frac{\partial^2 V_{1,F}^{th}}{\partial h^2}\Big|_{h=0} = \frac{T^2}{12}\frac{\partial^2}{\partial h^2} m_{N1}^2 = -\frac{T^2}{6}\frac{m_{N'}\,\mathrm{Re}(y_1 y_2)}{m_L}$$

Thus, $\frac{\partial^2 V_{1,F}^{th}}{\partial h^2}\Big|_{h=0} < 0$ is possible by choosing $\mathrm{Re}(y_1 y_2) > 0$.
$m_L^2 >> T^2$ is possible if new fermions gain their masses through some dynamical mechanism.

MODEL I: SINGLET-DOUBLET FERMIONS + REAL SCALAR SINGLET + SCALAR SINGLET WITH $O(N_\rho)$

$$L^i_{L,R} = \begin{bmatrix} N^i \\ E^i \end{bmatrix}_{L,R} \sim (1,2)_{-\frac{1}{2}},\ N'^i_{L,R} \sim (1,1)_0,\ E'^i_{L,R} \sim (1,1)_{-1}$$

$$\mathcal{L} = \mathcal{L}_{SM} + \sum_{i=1}^{N_F} \left(\mathcal{L}^i_{kin}(L, N', E') + \mathcal{L}^i_{yuk} \right) + \mathcal{L}_{kin}(\sigma, \rho) - V_0(\sigma, \rho)$$

$$\begin{aligned} \mathcal{L}^i_{yuk} =& - y^i_{NN'1} \overline{L^i_L} \widetilde{\phi} N'^i_R - y^i_{NN'2} \overline{N'^i_L} \widetilde{\phi}^\dagger L^i_R - y^i_{EE'1} \overline{L^i_L} \phi E'^i_R - y^i_{EE'2} \overline{E'^i_L} \phi^\dagger L^i_R \\ & - y^i_L \sigma \overline{L^i_L} L^i_R - y^i_{N'} \sigma \overline{N'^i_L} N'^i_R - y^i_{E'} \sigma \overline{E'^i_L} E'^i_R + h.c. \\ V_0(\sigma, \rho) =& - \frac{1}{2} \mu^2_\sigma \sigma^2 + \frac{1}{4} \lambda_\sigma \sigma^4 \\ & - \frac{1}{2} \mu^2_\rho \rho_i \rho_i + \frac{1}{4} \lambda_\rho \left(\rho_i \rho_i \right)^2 + \frac{1}{4} \lambda_{\sigma\rho} \sigma^2 \rho_i \rho_i \end{aligned}$$

The physical masses (for each copy of new fermions) are:

$$m_{N1}^2 = \frac{1}{2}\left(A_N^2 - \sqrt{\left(A_N^2\right)^2 - 4\left(\Delta_N^2\right)^2}\right)$$
$$m_{N2}^2 = \frac{1}{2}\left(A_N^2 + \sqrt{\left(A_N^2\right)^2 - 4\left(\Delta_N^2\right)^2}\right)$$

where

$$A_N^2 = |m_{NN'1}|^2 + |m_{NN'2}|^2 + |m_{N'}|^2 + |m_L|^2$$
$$\Delta_N^2 = |m_L m_{N'} - m_{NN'1} m_{NN'2}|$$
$$m_{NN'i} = \frac{1}{\sqrt{2}} y_{NN'i} h,\ \ (i = 1, 2)$$
$$m_x = y_x \sigma,\ \ (x = L, N', E')$$

m_{E1}, m_{E2} are same as equations above, except $N \to E$.

At high T, when $(y_L v_\sigma)^2 \gg T^2$,

$$\begin{aligned} \partial_h^2 V_1^{th}(h=0, v_\sigma) &= -a_h T^2 \,, \\ a_h &= \frac{N_F}{6y_L}\left(y_{N'} y_{NN'1} y_{NN'2} + y_{E'} y_{EE'1} y_{EE'2}\right) \\ &\quad - \left(\frac{3}{16} g^2 + \frac{1}{16} g'^2 + \frac{1}{4} y_t^2 + \frac{1}{2}\lambda_h\right) \,. \end{aligned}$$

- When $\frac{N_F}{6y_L}\left(y_{N'} y_{NN'1} y_{NN'2} + y_{E'} y_{EE'1} y_{EE'2}\right)$ is large enough, the negative contribution outweigh the usual positive contributions from SM particles, thus $\partial_h^2 V_{eff}(h=0, v_\sigma) < 0$, and $v_h \neq 0$ at high T.

$$\partial_\sigma^2 V_1^{th}(h=0,\sigma=0) = -a_\sigma T^2\,,$$
$$a_\sigma = -\frac{N_\rho}{24}\lambda_{\sigma\rho} - \frac{1}{4}\lambda_\sigma - \frac{N_F}{6}\left(2y_L^2 + y_{N'}^2 + y_{E'}^2\right)\,.$$

- To satisfy $(y_L v_\sigma)^2 \gg T^2$, we need large enough v_σ at high T too.
- $a_\sigma > 0$ guarantees that $v_\sigma \neq 0$ at high T. Although this condition is neither sufficient nor necessary, it helps us to obtain the correct benchmarks.
- $\lambda_{\sigma\rho} < 0$ and sufficiently large $N_\rho|\lambda_{\sigma\rho}|$ are required to satisfy $a_\sigma > 0$.

Model II: Singlet-doublet fermions + real scalar singlet + scalar singlet with $O(N_\rho)$ + inert Higgs doublet

$$V_0 = V_0(\Phi_1, \Phi_2) + V_0(\sigma, \rho) + \widetilde{V}_0$$

$$V_0(\Phi_1, \Phi_2) = -\mu_1^2 \Phi_1^\dagger \Phi_1 + \lambda_1 \left(\Phi_1^\dagger \Phi_1\right)^2 - \mu_2^2 \Phi_2^\dagger \Phi_2 + \lambda_2 \left(\Phi_2^\dagger \Phi_2\right)^2$$

$$\widetilde{V}_0 = \lambda_3 (\Phi_1^\dagger \Phi_1)(\Phi_2^\dagger \Phi_2) + \lambda_4 (\Phi_1^\dagger \Phi_2)(\Phi_2^\dagger \Phi_1) + \sum_{i=1}^{2} \left(\frac{1}{2} \lambda_{\sigma \Phi_i} \sigma^2 (\Phi_i^\dagger \Phi_i) + \frac{1}{2} \lambda_{\rho \Phi_i} (\rho_j \rho_j)(\Phi_i^\dagger \Phi_i) \right)$$

$$\mathcal{L}^i_{yuk} = - y^i_{NN'1} \overline{L^i_L} \widetilde{\Phi_2} N'^i_R - y^i_{NN'2} \overline{N'^i_L} \widetilde{\Phi_2}^\dagger L^i_R - y^i_{EE'1} \overline{L^i_L} \Phi_2 E'^i_R - y^i_{EE'2} \overline{E'^i_L} \Phi_2^\dagger L^i_R - y^i_L \sigma \overline{L^i_L} L^i_R - y^i_{N'} \sigma \overline{N'^i_L} N'^i_R - y^i_{E'} \sigma \overline{E'^i_L} E'^i_R + h.c.$$

$$a_h = \frac{N_F}{6 y_L} \left(y_{N'} y_{NN'1} y_{NN'2} + y_{E'} y_{EE'1} y_{EE'2} \right) - \left(\frac{3}{16} g^2 + \frac{1}{16} g'^2 + \frac{1}{2} \lambda_2 \right)$$

$$\Phi_j = \begin{bmatrix} \varphi_j^+ \\ (h_j + i\varphi_j^0)/\sqrt{2} \end{bmatrix}$$

At $T = 0$,

$$\langle \Phi_2 \rangle = \begin{bmatrix} 0 \\ 0 \end{bmatrix}$$

THERMAL HISTORIES

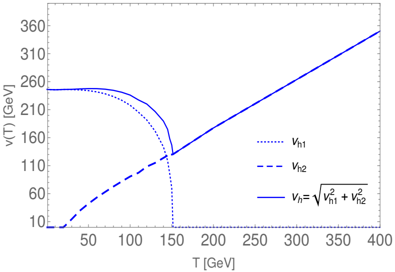

Thermal history in which the electroweak symmetry is always broken.

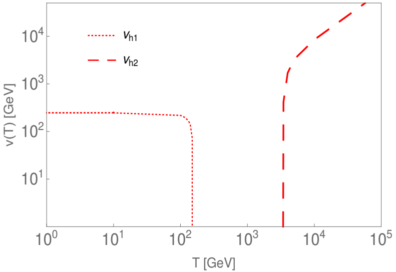

Thermal history in which the electroweak symmetry is only temporarily restored.

Thermal Histories

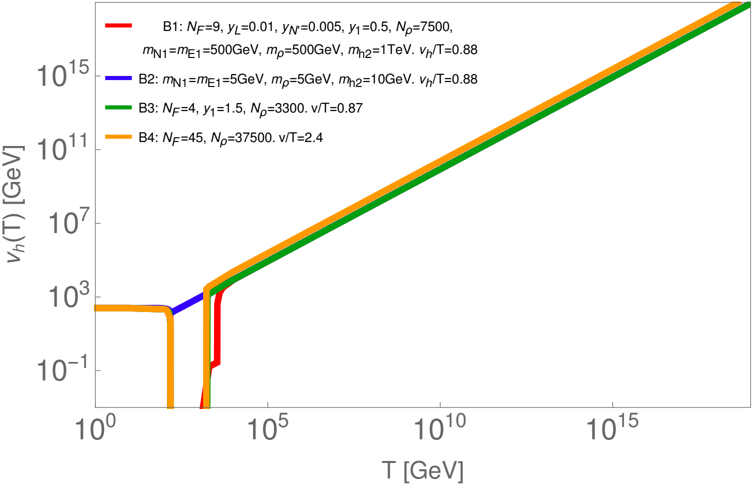

Temperature-dependent vev for several benchmarks.

Thermal histories

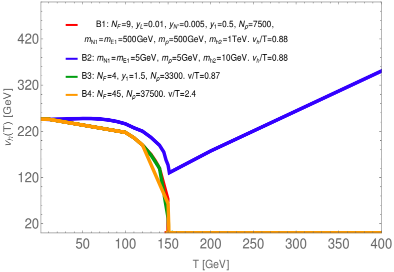

Lower temperature limits of temporary-restored phases.

- B1,B3,B4 have the same lower temperature limits of temporary-restored phases because SM-like Higgs does not couple with new fermions and and new scalars at tree-level.

THERMAL HISTORIES

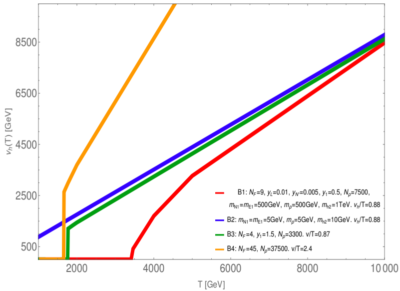

Upper temperature limits of temporary-restored phases.

- The value v_h/T of at high T depends on a_h.

THERMAL HISTORIES

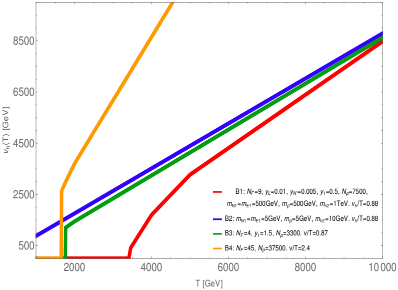

Upper temperature limits of temporary-restored phases.

- The value v_h/T of at high T depends on a_h.

$$\partial_h^2 V_{eff}(h=0, v_\sigma) \approx -a_h T^2 \,,$$

$$a_h = \frac{N_F}{6y_L}\left(y_{N'} y_{NN'1} y_{NN'2} + y_{E'} y_{EE'1} y_{EE'2}\right) - \left(\frac{3}{16}g^2 + \frac{1}{16}g'^2 + \frac{1}{2}\lambda_2\right) \,.$$

THERMAL HISTORIES

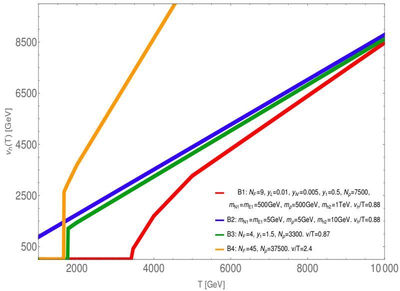

Upper temperature limits of temporary-restored phases.

- The value v_h/T of at high T depends on a_h.
- The length of temporary-restored phase depends on the masses of new fermions and new scalars (at $T = 0$), $N_\rho \lambda_\rho$, and a_h.

Thermal histories

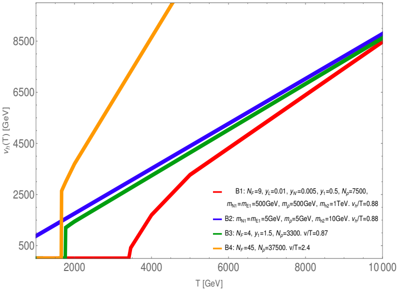

Upper temperature limits of temporary-restored phases.

- The value v_h/T of at high T depends on a_h.
- The length of temporary-restored phase depends on the masses of new fermions and new scalars (at $T = 0$), $N_\rho \lambda_\rho$, and a_h.
- Each temporary-restored phase starts with a second order phase transtion, and but can ends with either a first order or second order phase transition (depending on a_h).

RGEs and stability of V_{eff}

$$(4\pi)^2 \frac{d\lambda_2}{dt} = 24\lambda_2^2 + \frac{3}{8}\left(2g_2^4 + \left(g_2^2 + g'^2\right)^2\right) - \left(9g_2^2 + 3g'^2\right)\lambda_2$$
$$+ 2\lambda_3^2 + 2\lambda_3\lambda_4 + \lambda_4^2 + \frac{N_\rho}{2}\lambda_{\rho\Phi_2}^2 + \frac{1}{2}\lambda_{\sigma\Phi_2}^2$$
$$+ 2N_F\left(2\left(y_{NN'1}^2 + y_{NN'2}^2 + y_{EE'1}^2 + y_{EE'2}^2\right)\lambda_2 - \left(y_{NN'1}^4 + y_{NN'2}^4 + y_{EE'1}^4 + y_{EE'2}^4\right)\right)$$

$$(4\pi)^2 \frac{dg'}{dt} = (7 + 2N_F)\, g'^3$$

$$(4\pi)^2 \frac{dg_2}{dt} = \left(-3 + \frac{2}{3}N_F\right) g_2^3$$

$$(4\pi)^2 \frac{dy_{NN'1}}{dt} = 2y_{N'}y_L y_{NN'2} + y_{NN'1}\left[\frac{3}{2}y_{NN'1}^2 - \frac{3}{2}y_{EE'1}^2 + \frac{1}{2}y_{N'}^2 + \frac{1}{2}y_L^2\right.$$
$$\left. + N_F(y_{NN'1}^2 + y_{NN'2}^2 + y_{EE'1}^2 + y_{EE'2}^2) - \frac{9}{4}g_2^2 - \frac{3}{4}g'^2\right]$$

$$(4\pi)^2 \frac{d\lambda_\rho}{dt} = 2(N_\rho + 8)\lambda_\rho^2 + \frac{1}{2}\lambda_{\sigma\rho}^2 + 2\left(\lambda_{\rho\Phi_1}^2 + \lambda_{\rho\Phi_2}^2\right)$$

RGEs and stability of V_{eff}

$$(4\pi)^2 \frac{d\lambda_2}{dt} = 24\lambda_2^2 + \frac{3}{8}\left(2g_2^4 + \left(g_2^2 + g'^2\right)^2\right) - \left(9g_2^2 + 3g'^2\right)\lambda_2$$
$$+ 2\lambda_3^2 + 2\lambda_3\lambda_4 + \lambda_4^2 + \frac{N_\rho}{2}\lambda_{\rho\Phi_2}^2 + \frac{1}{2}\lambda_{\sigma\Phi_2}^2$$
$$+ 2N_F\left(2\left(y_{NN'1}^2 + y_{NN'2}^2 + y_{EE'1}^2 + y_{EE'2}^2\right)\lambda_2 - \left(y_{NN'1}^4 + y_{NN'2}^4 + y_{EE'1}^4 + y_{EE'2}^4\right)\right)$$

$$(4\pi)^2 \frac{dg'}{dt} = (7 + 2N_F)\, g'^3, \quad (4\pi)^2 \frac{dg_X}{dt} = -\frac{1}{3}\left(11N_X - 8n_F\right) g_X^3$$

$$(4\pi)^2 \frac{dg_2}{dt} = \left(-3 + \frac{2}{3}N_F\right) g_2^3$$

$$(4\pi)^2 \frac{dy_{NN'1}}{dt} = 2y_{N'}y_L y_{NN'2} + y_{NN'1}\left[\frac{3}{2}y_{NN'1}^2 - \frac{3}{2}y_{EE'1}^2 + \frac{1}{2}y_{N'}^2 + \frac{1}{2}y_L^2\right.$$
$$\left. + N_F(y_{NN'1}^2 + y_{NN'2}^2 + y_{EE'1}^2 + y_{EE'2}^2) - \frac{9}{4}g_2^2 - \frac{3}{4}g'^2 - 3\left(N_X - \frac{1}{N_X}\right) g_X^2\right]$$

$$(4\pi)^2 \frac{d\lambda_\rho}{dt} = 2(N_\rho + 8)\lambda_\rho^2 + \frac{1}{2}\lambda_{\sigma\rho}^2 + 2\left(\lambda_{\rho\Phi_1}^2 + \lambda_{\rho\Phi_2}^2\right)$$

(N, N', E, E' are charged under $SU(N_X)$. $N_F = N_x\, n_F$.)

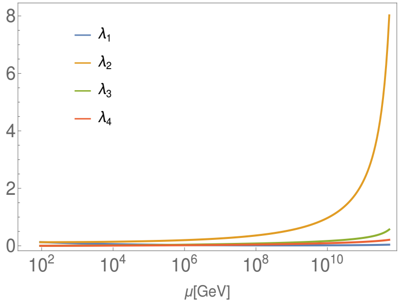

B1: $n_F = 3, \quad N_x = 3.$

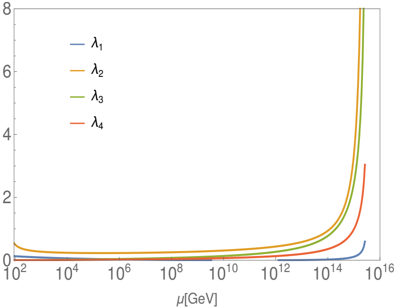

B5: $n_F = 1, \quad N_x = 4.$

The effective potential is stable, and the quartic couplings λ_i stays perturbative over a large range of energy scales.

Requiring all couplings stays perturbative up to 10^{10} GeV implies:

- $$g' \quad \text{stays perturbative} \quad \Rightarrow N_F \leq 12$$
- $$\lambda_\rho \quad \text{stays perturbative} \quad \Rightarrow N_\rho \lambda_\rho \lesssim 1.5$$
- $$\frac{y_L v_\sigma}{T} \gtrsim 4, \quad a_\sigma \gtrsim 0, \quad \lambda_\sigma \geq \frac{1}{\lambda_\rho}\left(\frac{\lambda_{\sigma\rho}}{2}\right)^2 \Rightarrow N_\rho \gtrsim \frac{64}{|x_{min}|} N_F$$

  x_{min} is the minimum of $f(x) = \frac{\pi^2}{2} x^2 + N_\rho \lambda_\rho J_B(x)$. E.g. choosing $N_\rho \lambda_\rho = 1.5$ implies $N_\rho \gtrsim 552 N_F$.
- $$\lambda_2 > 0 \Rightarrow \lambda_2 \gtrsim y_{NN'1}^2/2$$

  (assume $y_{NN'1} = y_{NN'2} = y_{EE'1} = y_{EE'2}$ at $T = 0$)
- $$y_{NN'i}, y_{EE'i} \quad \text{stays perturbative} \quad \Rightarrow \left(N_X - \frac{1}{N_X}\right) g_X^2 \gtrsim \frac{4}{3} N_F y_{NN'1}^2$$

BENCHMARKS

n_F	4	3	3	1
N_X	3	3	2	4
$y_{NN'i} = y_{EE'i}$	0.4	0.5	0.75	1.5
$y_{N'}$	0.005	0.005	0.005	0.005
$y_{L'}$	0.01	0.01	0.01	0.01
m_{N1}(GeV)	500	500	500	500
N_ρ	8500	7500	8500	8500
$\lambda_{\sigma\rho}$	-1.2×10^{-6}	-1.2×10^{-6}	-1.2×10^{-6}	-1.2×10^{-6}
λ_2	0.081	0.126	0.28	0.54
m_{h2}(GeV)	1000	1000	1000	1000
m_ρ(GeV)	500	500	500	500
g_X	1	1.1	1.64	$\sqrt{4\pi}$

$$N_\rho \lambda_\rho = 1.5, \quad \lambda_\sigma = \frac{1}{\lambda_\rho} \left(\frac{\lambda_{\sigma\rho}}{2} \right)^2$$

SUMMARY AND OUTLOOK

- EWSNR can be induced by new fermions from renormalizable models.
- The parameter spaces of these models are tightly constrained by theoretical constraints.
- Intriguing cosmological implications: origin of matter-antimatter asymmetry (suppressed sphaleron rate), early matter dominated era?

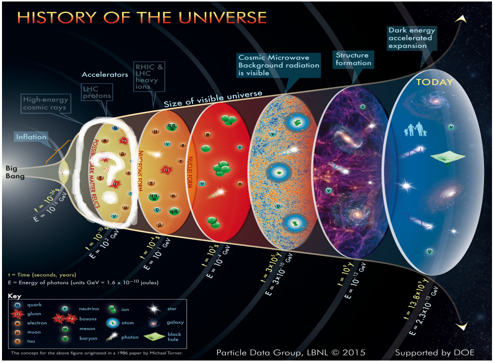

EFFECTIVE POTENTIAL

- Effective potential

$$V_{eff} = V_0 + \sum_i \left(V_i^{CW} + V_{1,i}^{th} + V_{ring,i}^{th} \right)$$

- Tree-level potential:

$$V_0 = V_0(\Phi_1, \Phi_2) + V_0(\sigma, \rho) + \widetilde{V}_0$$

$$V_0(\Phi_1, \Phi_2) = -\mu_1^2 \Phi_1^\dagger \Phi_1 + \lambda_1 \left(\Phi_1^\dagger \Phi_1 \right)^2 - \mu_2^2 \Phi_2^\dagger \Phi_2 + \lambda_2 \left(\Phi_2^\dagger \Phi_2 \right)^2$$

$$\widetilde{V}_0 = \lambda_3 (\Phi_1^\dagger \Phi_1)(\Phi_2^\dagger \Phi_2) + \lambda_4 (\Phi_1^\dagger \Phi_2)(\Phi_2^\dagger \Phi_1) + \sum_{i=1}^{2} \left(\frac{1}{2} \lambda_{\sigma\Phi_i} \sigma^2 (\Phi_i^\dagger \Phi_i) + \frac{1}{2} \lambda_{\rho\Phi_i} (\rho_j \rho_j)(\Phi_i^\dagger \Phi_i) \right)$$

$$V_0(\sigma, \rho) = -\frac{1}{2} \mu_\sigma^2 \sigma^2 + \frac{1}{4} \lambda_\sigma \sigma^4 - \frac{1}{2} \mu_\rho^2 \rho_i \rho_i + \frac{1}{4} \lambda_\rho \left(\rho_i \rho_i \right)^2 + \frac{1}{4} \lambda_{\sigma\rho} \sigma^2 \rho_i \rho_i$$

(*Please see hep-ph/9901312 for more details.*)

- Coleman-Weinberg potential (for i-th particle)

$$V_i^{CW} = (-1)^{a_i} n_i \frac{m_i^4}{64\pi^2}\left[\log\left(\frac{m_i^2}{\mu^2}\right) - c_i\right]$$

- One-loop thermal potential (for i-th particle)

$$V_{1,i}^{th} = (-1)^{a_i} n_i \frac{T^4}{2\pi^2} J_{B/F}\left(\frac{m_i^2}{T^2}\right)$$

$$J_{B/F}(y^2) = \int_0^\infty dx\, x^2 \log\left[1 \mp \exp\left(-\sqrt{x^2+y^2}\right)\right]$$

- Daisy contribution (for i-th particle)

$$V_{ring,i}^{th} = \overline{n_i}\frac{T^4}{12\pi}\left[\left(\frac{m_i^2}{T^2}\right)^{3/2} - \left(\frac{\mathcal{M}_i^2}{T^2}\right)^{3/2}\right]$$

THERMAL CORRECTIONS BEYOND ONE LOOP

$$V_1^{th}(\phi, T) = \sum_i \frac{n_i T}{2} \sum_{-\infty}^{\infty} \int \frac{d^3\vec{k^2}}{(2\pi)^3} \log\left[\vec{k}^2 + \omega_n^2 + m_i^2(\phi)\right]$$

$$= \sum_i (-1)^{a_i} n_i \frac{T^4}{2\pi^2} J_{B/F}\left(\frac{m_i^2}{T^2}\right)$$

$$V_{ring}^{th}(\phi, T) = \sum_i \frac{\bar{n}_i T}{12\pi}\left[m_i^3(\phi) - \mathcal{M}_i^3(\phi, T)\right]$$

$$\omega_n = 2n\pi T \ (bosons), (2n+1)\pi T \ (fermions)$$

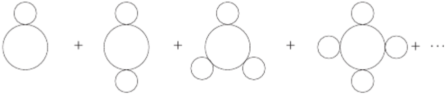

Figure 2: Some generic examples of ring diagrams where each solid line may represent either a scalar, a fermion or a gauge field. The small loops correspond to thermal loops in the IR limit. They are all separately IR divergent, but their sum is IR finite.

$\mathcal{M}_i^2(\phi, T) = m_i^2(\phi) + \Pi_i(\phi, T)$ (except $i = Z_L, \gamma_L$).

Truncated Full Dressing Method:

$$\begin{aligned}
\Pi_h(\phi,T) &= \left(\frac{3g^2+g'^2}{16}+\frac{\lambda}{2}+\frac{y_t^2}{4}\right)T^2 = \Pi_\chi(\phi,T) \ , \\
\Pi_{W_L}(\phi,T) &= \frac{11}{6}g^2T^2 \ , \\
\Pi_{W_T}(\phi,T) &= \Pi_{Z_T}(\phi,T) = \Pi_{\gamma_T}(\phi,T) = 0 \ , \qquad \text{(A14)} \\
\mathcal{M}^2_{Z_L}(\phi) &= \frac{1}{2}\left[m_Z^2(t) + \frac{11}{6}\frac{g^2}{\cos^2\theta_W}T^2 + \Delta(\phi,T)\right] \ , \\
\mathcal{M}^2_{\gamma_L}(\phi) &= \frac{1}{2}\left[m_Z^2(t) + \frac{11}{6}\frac{g^2}{\cos^2\theta_W}T^2 - \Delta(\phi,T)\right] \ , \\
& \qquad \text{(A15)}
\end{aligned}$$

Optimized Partial Dressing Method:

$$\delta m^2_{\phi_j}(h,T) = \sum_i \frac{\partial}{\partial \phi_j}\left[\frac{\partial V^i_{\rm CW}}{\partial \phi_j}\Big(m_i^2(h) + \delta m_i^2(h,T)\Big) + \frac{\partial V^i_{\rm th}}{\partial \phi_j}\Big(m_i^2(h) + \delta m_i^2(h,T), T\Big)\right] \quad \text{(A.1)}$$

$$\delta m_j^2(h,T) \approx \delta m^2_{j(a)} + (h - h_a)\frac{\partial \delta m^2_{j(a)}}{\partial h} \quad \text{(A.2)}$$

$$V^{\rm pd}_{\rm eff}(h,T) = V_0 + \sum_i \int dh \left[\frac{\partial V^i_{\rm CW}}{\partial h}\Big(m_i^2(h) + \delta m_i^2(h,T)\Big) + \frac{\partial V^i_{\rm th}}{\partial h}\Big(m_i^2(h) + \delta m_i^2(h,T), T\Big)\right], \quad \text{(A.4)}$$

Daisy and Super-Daisy contributions to thermal mass

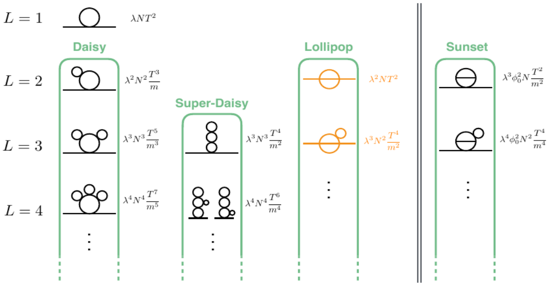

Figure 2. Complete set of 1- and 2- loop contributions to the scalar mass, as well as the most important higher loop contributions, in ϕ^4 theory. The scaling of each diagram in the high-temperature approximation is indicated, omitting symmetry- and loop-factors. Diagrams to the right of the vertical double-lines only contribute away from the origin when $\langle\phi\rangle = \phi_0 > 0$. We do not show contributions which trivially descend from e.g. loop-corrected quartic couplings. Lollipop diagrams (in orange) are not automatically included in the resummed one-loop potential.

Curtin, Meade & Ramani, arXiv:1612.00466

V_{eff} IN SM

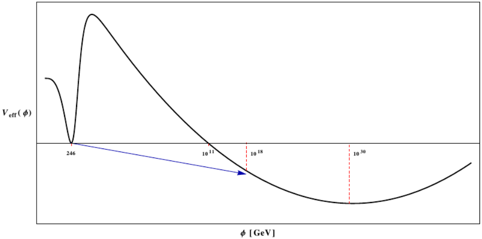

FIG. 2: The potential in the Standard Model, for $M_H = 125.7$ GeV and $M_t = 173.34$ GeV, is sketched (figure not to scale). The potential goes negative at a scale of 10^{11} GeV and reaches a new minimum at roughly 10^{30} GeV. The tunneling through the barrier goes from the base of the arrow ($\phi(r = \infty)$) to the tip ($\phi(0)$), which turns out to be close to or above the Planck scale.

Branchina, Messina & Sher, arXiv:1408.5302

STABILITY OF V_{eff} IN SM AND SINGLET-DOUBLET MODEL

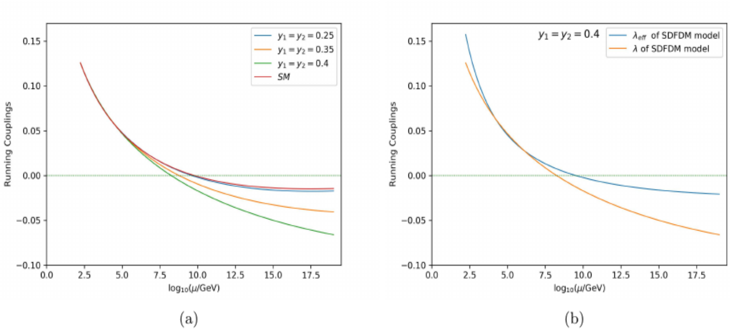

FIG. 1. (a) $\lambda(t)$ up to M_{Pl} for the SM and for various Yukawa couplings in the SDFDM model; (b) Running $\lambda(t)$ and $\lambda_{eff}(t)$ up to M_{Pl} scale for the SDFDM model.

Cheng & Liao, arXiv:1909.11941

Metastable Vacuum vs True Vacuum

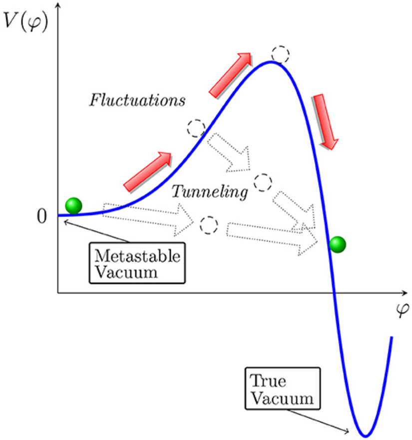

Markkanen, Rajantie & Stopyra, arXiv:1809.06923

In SM:

$$\tau = \left[\frac{R_M^4}{T_U^4}\, e^{\frac{8\pi^2}{3|\lambda(\mu)|}}\right] \times \left[e^{\Delta S}\right] \times T_U$$

$$R_M \sim 1.87 \cdot 10^{-17}\, GeV^{-1} = 224.5\, M_P^{-1}$$

$$\lambda(1/R_M) = -0.01345\,,$$

$$\tau_{tree} \sim 10^{613}\, T_U$$

$$
\begin{aligned}
(4\pi)^2 \frac{d\lambda_1}{dt} &= 24\lambda_1^2 - 6y_t^4 + \frac{3}{8}\left(2g_2^4 + \left(g_2^2 + g'^2\right)^2\right) + \left(12y_t^2 - 9g_2^2 - 3g'^2\right)\lambda_1 \\
&\quad + 2\lambda_3^2 + 2\lambda_3\lambda_4 + \lambda_4^2 + \frac{N_\rho}{2}\lambda_{\rho\Phi_1}^2 + \frac{1}{2}\lambda_{\sigma\Phi_1}^2 \\
(4\pi)^2 \frac{dg_3}{dt} &= -7g_3^3
\end{aligned}
$$

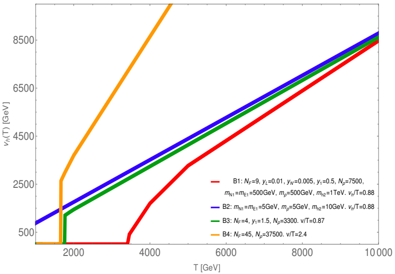

Upper temperature limits of temporary-restored phases.

Table 1. Frequency classification of gravitational waves and their detection method [4-6]

Frequency band	Detection method
Ultra high frequency band: above 1 THz	Terahertz resonators, optical resonators, and magnetic conversion detectors
Very high frequency band: 100 kHz–1 THz	Microwave resonator/wave guide detectors, laser interferometers and Gaussian beam detectors
High frequency band (audio band)*: 10 Hz–100 kHz	Low-temperature resonators and ground-based laser-interferometric detectors
Middle frequency band: 0.1 Hz–10 Hz	Space laser-interferometric detectors of arm length 100 km − 60,000 km, atom and molecule interferometry, optical clock detectors
Low frequency band (milli-Hz band)†: 100 nHz–0.1 Hz	Radio Doppler tracking of spacecraft, space laser-interferometric detectors of arm length longer than 60,000 km, optical clock detectors
Very low frequency band (nano-Hz band): 300 pHz – 100 nHz	Pulsar timing arrays (PTAs)
Ultralow frequency band: 10 fHz–300 pHz	Astrometry of quasars and their proper motions
Extremely low (Hubble) frequency band (cosmological band): 1 aHz–10 fHz	Cosmic microwave background experiments
Beyond Hubble-frequency band: below 1 aHz	Through the verifications of inflationary/primordial cosmological models

*The range of audio band (also called LIGO band) normally goes only to 10 kHz.
†The range of milli-Hz band is 0.1 mHz to 100 mHz.

arXiv:1709.05659